THE JOURNAL OF PHYSICAL CHEMISTRY A

pubs.acs.org/JPCA Article

Autoinhibition by Iodide Ion in the Methionine–Iodine Reaction

Li Xu, György Csekő, and Attila K. Horváth*

Cite This: J. Phys. Chem. A 2020, 124, 6029–6038 Read Online

ACCESS | Metrics & More | Article Recommendations | Supporting Information

ABSTRACT: The methionine–iodine reaction was reinvestigated spectrophotometrically in detail monitoring the absorbance belonging to the isosbestic point of iodine at 468 nm, at T = 25.0 ± 0.1 °C, and at 0.5 M ionic strength in buffered acidic medium. The stoichiometric ratio of the reactants was determined to be 1:1 producing methionine sulfoxide as the lone sulfur-containing product. The direct reaction between methionine and iodine was found to be relatively rapid in the absence of initially added iodide ion, and it can conveniently be followed by the stopped-flow technique. Reduction of iodine eventually leads to the formation of iodide ion that inhibits the reaction making the whole system autoinhibitory with respect to the halide ion. We have also shown that this inhibitory effect appears quite prominently, and addition of iodide ion in the millimole concentration range may result in a rate law where the formal kinetic order of this species becomes −2. In contrast to this, hydrogen ion has just a mildly inhibitory effect giving rise to the fact that iodine is the kinetically active species in the system but not hypoiodous acid. The surprisingly complex kinetics of this simple reaction may readily be interpreted via the initiating rapidly established iodonium-transfer process between the reactants followed by the subsequent hydrolytic decomposition of the short-lived iodinated methionine. A seven-step kinetic model to be able to describe the most important characteristics of the measured kinetic curves is established and discussed in detail.

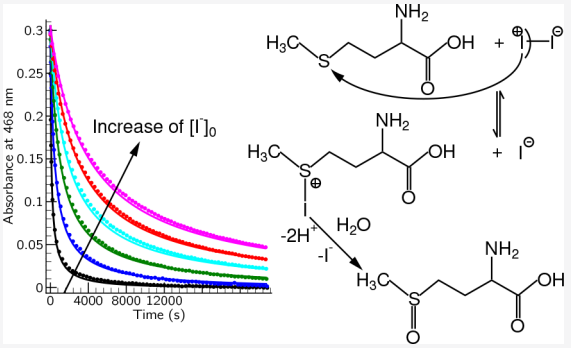

INTRODUCTION

Sulfur-containing amino acids are not only important sources of sulfur nutrients in humans and mammals[1] but also play an important role in various biochemical processes such as transformation and synthesis of proteins,[2] immunity,[3,4] as well as oxidative stress resistance.[5−7] It is generally considered that redox reaction balance of many sulfur-containing amino acids is closely associated with cardiovascular disease, neuropsychiatric disorder, neurogenic diseases, renalischemia, liver failure, diabetes, cancer, and aging.[1,6,8−12] The sulfur-containing amino acids supplementation may readily scavenge biological reactive oxidants *in vivo* through their redox reactions to protect the stability and activity of other essential amino acids in proteins reducing the damage to cell membrane and DNA caused by oxidative stress and, in turn, incidence of these diseases.

Methionine (Met), as one of two essential sulfur-containing amino acids, may be obtained only from the human diet. Met is not only a precursor in protein synthesis but also participates in many biochemical processes,[3,8,13,14] such as glycogen and D-glucose formation, production of *S*-adenosylmethionine and Succinyl-CoA, biosynthesis of homocysteine, cysteine, and glutathione, metabolism of phosphatidylcholine and phospholipids, as well as cellular and DNA methylation. In addition, it is found that Met in proteins is highly susceptible to oxidation under oxidative stress.[15−19] As an antioxidant defense system, Met oxidation participates in regulation of protein stability[20] and cellular viability[21] through its own oxidation: Met is oxidized to form methionine sulfoxide(MetSO) by adding oxygen to its sulfur atom in the physiological environment. MetSO produced may easily be reduced back to Met by thioredoxin-dependent enzymes under catalysis of methionine sulfoxide reductase.[7,22] The impairment of this regulation is associated with many diseases such as lung disease,[23] cancer,[24] neurodegeneration (Alzheimer's disease),[25] and cardiovascular and cerebrovascular disease.[26,27] However, the regulation functions of methionine as an antioxidant are still not fully explored. In order to understand the relationship between its oxidation process and biological regulation function, it is crucial to perform further investigations on the mechanism of methionine oxidation.

Sulfur-containing amino acids have three possible coordination sites including oxygen, nitrogen, and sulfur parts, and among them, the sulfur site is believed to be the most likely to be attacked by electrophilic agents due to its abundant electron density. Several investigations on the kinetics and mechanism of oxidation of methionine by different biological oxidants have

Received: May 12, 2020
Revised: June 25, 2020
Published: June 25, 2020

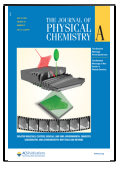

https://dx.doi.org/10.1021/acs.jpca.0c04271
J. Phys. Chem. A 2020, 124, 6029–6038

been reported with numerous oxidizing agents like metal ions,[28−30] halogen-containing inorganic oxidants,[31−33] hydrogen peroxide,[34,35] hydroxyl radicals,[36] and halogenated organic oxidants.[13,37−39] Even though most of these studies showed that the reaction is first order with respect to both methionine and the oxidant and methionine is oxidized to methionine sulfoxide as a final product, transient species during the course of reaction and their pathways are still not completely revealed. Taking the oxidation of methionine with halogen-containing oxidants as examples, the studies[31,32,37,39] showed that the methionine was first halogenated to give halosulfonium cation followed by the formation of methionine sulfoxide through the sequence of fast reactions. However, the reaction pathways from halosulfonium cation to methionine sulfoxide are different: Armesto,[31] Chikwana,[32] and Goyal[39] showed methionine sulfoxide is formed by the hydrolysis of halosulfonium cation, while Gangwani[37] indicated that the halosulfonium cation is highly solvated to give final product. In addition, the earlier results give evidence for a tetracoordinated sulfurane intermediate and reaction product, cyclic sulfinine dehydromethionine.[40] Recently, Diculescu[41] pointed out that methionine oxidation leads to methionine sulfoxide by hydrolysis of dehydromethionine intermediate. Instead of product, methionine sulfoxide could be an intermediate to react further with a second oxidant molecule to form a complex yielding the end-product, sulfone, by a series of fast steps.[13] Moreover, a theoretical study on the oxidation of methionine by hydroxyl radicals predicted that α-aminoalkyl radical is the intermediate proceeding to the final product, thioether aldehyde.[36] The important role of methionine in biochemical processes highlighted above as well as its diverse transformation to various sulfur-containing intermediates and products awaits for comprehensive and detailed kinetic studies to unravel the intimate nature of this essential amino acid to redox processes.

EXPERIMENTAL SECTION

Materials. All chemicals including iodine, DL-methionine, phosphoric acid, sodium dihydrogen phosphate, potassium iodide, and sodium perchlorate were of the commercially available highest purity and used without further purification. The corresponding stock solutions were prepared from twice ion-exchanged and two times atmospherically distilled water over potassium permanganate to avoid any organic or inorganic impurities originating from the exchange resin. The pH of buffer solutions was adjusted to be in the range of 1.60 and 2.60 by using phosphoric acid and dihydrogen phosphate taking the pK_a of phosphoric acid to be 1.8.[42] The pK_{a1} of methionine was also taken into consideration as 2.28.[42] The concentration of dihydrogen phosphate was kept constant at 0.3 M, and the ionic strength was kept at 0.5 M in all reactions by adding the necessary amount of sodium perchlorate as the background electrolyte. The methionine and potassium iodide solutions were freshly prepared before each experiment. The concentration of iodine in the stock solution was determined with iodometric method and checked with a UV−vis spectrometer as well before each measurement. The temperature of reaction cell was maintained at 25.0 ± 0.1 °C by thermostatting the cell holder with a water-circulating bath. Some experiments were performed in the absence of initially added iodide ion; however, $[I^-]_0$ in the majority of the kinetic measurements was kept constant at 0.003 M, except those ones where the effect of initially added iodide ion was investigated. Initial concentration of iodine and methionine were varied in the range of 0.120−25.01 mM and 0.067−0.872 mM, respectively

Methods and Instrumentation. The kinetic runs in the presence of initially added iodide ion were monitored by an Analytik Jena Specord S600 diode array spectrophotometers in the wavelength range of 400−900 nm. The deuterium lamp of the photometer was switched off during the whole course of experiments to avoid any undesired photochemically induced side effect of the UV radiation. The reaction was carried out in a standard quartz cuvette having a 1 cm optical path and equipped with a magnetic stirrer bar and a closely sealed Teflon cap. The buffer solution followed by the iodide and iodine solutions were delivered into the cuvette from a pipet first, and the spectrum of the solution was always recorded before initiation of the reaction to determine the exact initial iodine concentration. The reaction was then triggered by rapidly adding a necessary amount of methionine stock solution. Several repeated experiments have also been carried out indicating a good reproducibility of the kinetic measurement (see Figure S1 in the Supporting Information).

The reaction without initially added iodide ion at high excess of methionine was found to be too fast to be studied by S600 diode array spectrophotometer. Therefore, at these conditions the reaction was followed at 468 nm wavelength by an Applied Photophysics SX20 stopped-flow instrument equipped with a monochromator. The optical path was set to 1 cm, and the dead-time of the stopped-flow instrument was determined to be 1.3 ms by a standard methodology as described previously.[43] Each single kinetic run was repeated five times, and then the average of those runs were used for data evaluation.

The stoichiometric studies of this reaction were carried out in an excess of iodine with and without initially added iodide. The concentration of iodine at the end of reaction was calculated from the absorbance determined by visible spectroscopy when reaction was completely finished. The ^{1}H NMR spectra of end products and DL-methionine were confirmed by a Bruker Avance III 500 spectrometer at 500 MHz. ^{1}H spectra were recorded in D_2O, and the chemical shifts are reported in ppm relative to solvent residual peak (4.79 ppm ^{1}H).[44]

Data Treatment. Because iodine and triiodide ion were found to be the only absorbing species in the visible region, the 468 nm wavelength, which is the isosbestic point of iodine and triiodide ion system, was selected for the data evaluation of the kinetic parameter performed by the comprehensive program package ChemMech/Zita.[45] During the whole calculation process pH = $-\log[H^+]$ is considered and the molar absorbance of iodine and triiodide ion was set to be 750 $M^{-1}cm^{-1}$.[46] Since each experimental kinetic curve originally contained more than 500 absorbance−time data pairs, it was necessary to reduce the number of data points at about 60−80 in each runs to avoid the unnecessarily long and time-consuming evaluation process. A total number of almost 11 500 experimental data obtained from 151 kinetic curves were used for simultaneous data evaluation procedure. A relative fitting method has been chosen to minimize the average deviation between the measured and calculated data. The criterion was that the average deviation approached 1.5%, which is quite close to the experimentally achievable limit of error. The initial conditions can be seen in Table S1 in the Supporting Information.

https://dx.doi.org/10.1021/acs.jpca.0c04271
J. Phys. Chem. A 2020, 124, 6029−6038

RESULTS

Stoichiometry. Any reliable kinetic studies should begin with unraveling the stoichiometry of the given process at the experimental condition studied. A suitable and conceivable method seems to be visible-spectroscopy for determination of the consumed iodine/methionine ratio (SR defined as $([I_2]_0 - [I_2]_\infty)/[Met]_0$) in excess of iodine. Table 1 displays some

Table 1. Experimental (SR) Defined as $([I_2]_0 - [I_2]_\infty)/[Met]_0$ in Excess of Iodine with and without Initially Added Iodide Ion

$[I_2]_0$/mM	$[Met]_0$/mM	$[I^-]_0$/mM	pH	A_∞ at 468 nm	SR
0.938	0.399	0.0	1.85	0.4135	0.97
0.868	0.399	0.0	1.85	0.3620	0.97
0.804	0.399	0.0	1.85	0.3106	0.98
0.731	0.399	0.0	1.85	0.2602	0.96
0.670	0.399	0.0	1.85	0.2127	0.97
0.596	0.399	0.0	1.85	0.1601	0.96
0.483	0.120	3.0	1.85	0.2740	0.98
0.483	0.210	3.0	1.85	0.2050	1.00
0.483	0.300	3.0	1.85	0.1370	1.00
0.483	0.390	3.0	1.85	0.0730	0.99
0.484	0.120	3.0	2.60	0.2720	1.01
0.484	0.240	3.0	2.60	0.1830	1.00
0.484	0.361	3.0	2.60	0.0980	0.98
0.560	0.299	1.0	2.60	0.1977	0.98
0.561	0.299	3.0	2.60	0.2007	0.98
0.558	0.299	5.0	2.60	0.2012	0.97
0.559	0.299	7.0	2.60	0.2016	0.97
0.558	0.299	9.0	2.60	0.2010	0.97
0.561	0.299	11.0	2.60	0.1990	0.99

examples of the calculated stoichiometric ratio; the rest of them may be found in Table S2 of the Supporting Information. As it can easily be seen, SR values indicate a stoichiometric ratio to be pretty close to 1.0 within the limit of experimental error. It appears to suggest that the following equation describes the stoichiometry of methionine−iodine reaction:

$$Met + I_2 + H_2O \rightarrow MetSO + 2I^- + 2H^+ \quad (1)$$

Besides methionine sulfoxide,[29,35] methionine sulfone[13,35] may also be a possible product upon oxidizing the sulfur center in methionine suggesting another possible limiting stoichiometry, but evidently under our experimental condition methionine sulfone cannot be formed in detectable amount.

$$Met + 2I_2 + 2H_2O \rightarrow MetSO_2 + 4I^- + 4H^+ \quad (2)$$

To support this statement, we have performed ^{1}H NMR studies to analyze the products in slight excess of methionine. Figure 1 shows a strong singlet peak around 2.1 ppm chemical shift belonging to the hydrogens of the *S*-methyl group of methionine, a triplet at around 2.6 ppm belonging to the methylene group of hydrogens adjacent to the sulfur atom and a triplet at around 3.8 ppm belonging to the hydrogen of the methine group. As it is seen, the most intense peak belongs to the S-methyl group which is suitable to identify the slight excess methionine after the reaction ended. For the sake of completeness, it should be mentioned that the most intense peak of the S-methyl group of methionine sulfoxide and methionine sulfone may be observed at around 2.75 and 3.15 ppm, respectively.[32] As it is seen, the NMR-spectrum of the

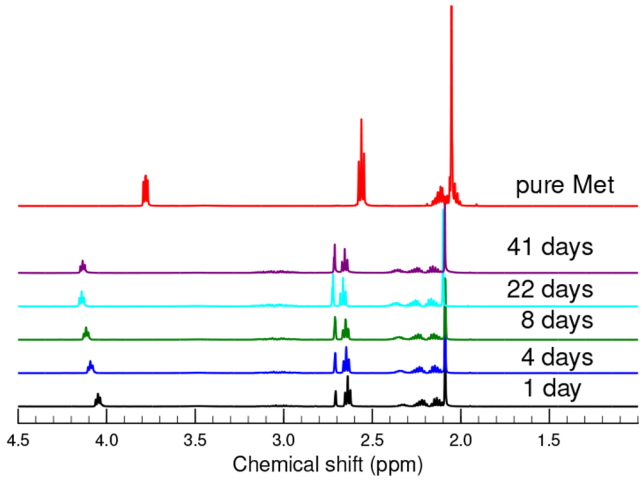

Figure 1. ^{1}H NMR spectrum of pure methionine and the product of the reaction at acidic medium. Conditions are as follows: 99.41 mM for pure methionine; 52.94 mM methionine, and 49.97 mM iodine for the reaction.

reaction mixture does not contain any observable peak in the 2.8−3.9 ppm region meaning that methionine sulfone cannot be the end-product of the title reaction. At the same time around 2.7 ppm, a singlet peak appears belonging to the methyl group of methionine sulfoxide. This latter peak is very stable for even over a month. Consequently, the stoichiometry of the title reaction can unambiguously be described by eq 1.

Initial Rate Studies. As it was mentioned in the introduction, there is no detailed kinetic study on the title reaction just a single subsection is devoted to unravel some characteristics, even though it is an essential and complex subsystem of the methionine−iodate clock reaction investigated by Chikwana et al.[32] It is known from their study that the formal kinetic order of methionine is 1 and that of iodide ion is −1 indicating an autoinhibitory behavior, but no information is available about those of iodine and hydrogen ion. Figure 2 represents the results of our study providing inevitable evidence that the kinetic orders of the reactants

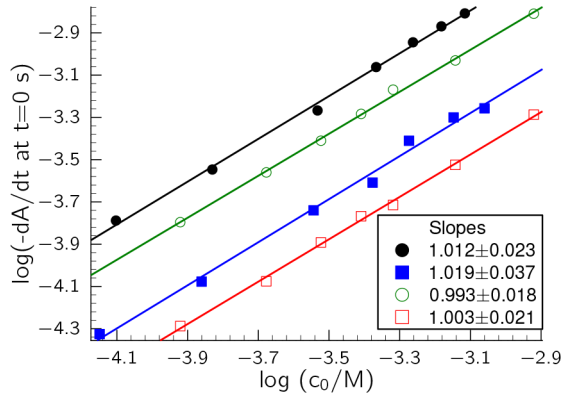

Figure 2. Initial rate studies to determine the formal kinetic orders of iodine (filled symbols) and methionine (empty symbols). Experimental conditions are as follows: (black circles) $[Met]_0$ = 0.48 mM, pH = 2.60, $[I^-]_0$ = 3.0 mM; (blue squares) $[Met]_0$ = 0.4 mM, pH = 2.10, $[I^-]_0$ = 3.0 mM, and c_0 values belong to initial total iodine concentrations. (green circles) T_{I_2} = 0.48 mM, pH = 2.35, $[I^-]_0$ = 3.0 mM; (red squares) T_{I_2} = 0.48 mM, pH = 1.60, $[I^-]_0$ = 3.0 mM.

https://dx.doi.org/10.1021/acs.jpca.0c04271
J. Phys. Chem. A 2020, 124, 6029−6038

(methionine and iodine) are strictly one. Furthermore, displaying the log−log plots of the initial rate versus concentration of iodide and hydrogen ion (shown in Figure 3) reveals a quite complex dynamical feature. As it is seen, both

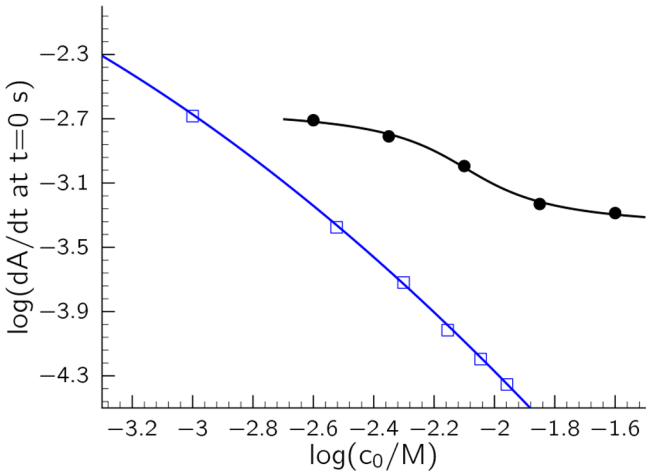

Figure 3. Log−log plots of initial rates against iodide and hydrogen ion concentrations. Conditions are as follows: (black circles) $[Met]_0$ = 1.2 mM, T_{I_2} = 0.48 mM, $[I^-]$ = 3.0 mM, and c_0 corresponds to $[H^+]$; (blue squares) $[Met]_0$ = 0.48, T_{I_2} = 0.48 mM, pH = 2.1, and c_0 corresponds to $[I^-]_0$.

plots indicate nonlinear dependence of the corresponding logarithmic concentration values. In the case of iodide, the result presented here contradicts with the formal kinetic order of iodide reported previously.[32] As we shall later show, it is the consequence of the limited concentration range of iodide ion used in Chikwana's experiments. It also means that the autoinhibitory feature of iodide ion is not as mild as mentioned in Chikwana's report. Actually, at slightly higher iodide concentrations, a strong second order inhibiting effect may easily be realized as we shall point out later. The sigmoid type of log−log plots shown in Figure 3 confirms that hydrogen ion has a very complex effect, hydrogen ion indeed inhibits the reaction as well, although this inhibition is not so effective. It is interesting to note that such a complex effect of hydrogen ion is not yet recognized previously.[32]

Individual Evaluation of Kinetic Curves. Our preliminary experiments measured in the absence of initially added iodide ion revealed that the reaction can be monitored by stopped-flow technique. However, even in huge excess of methionine the kinetic traces cannot be described by a single exponential behavior, thus our stopped-flow measurements are fully consistent to those ones reported in Chikwana's paper.[32] Such typical absorbance−time traces are visualized in Figure 4. The reason for this deviation may easily be interpreted in terms of the autoinhibitory effect of iodide ion. It should, however, be emphasized that this autoinhibition has to be strong enough to slow down the rate of conversion at the end of reaction, which means, indeed, more pronounced negative feedback effect of iodide than considered in Chikwana's paper. Taking into consideration of all these information obtained, we have performed individual evaluation of kinetic curves by considering the stoichiometry as eq 1 with a rate equation of taking into consideration eq 5 as well.

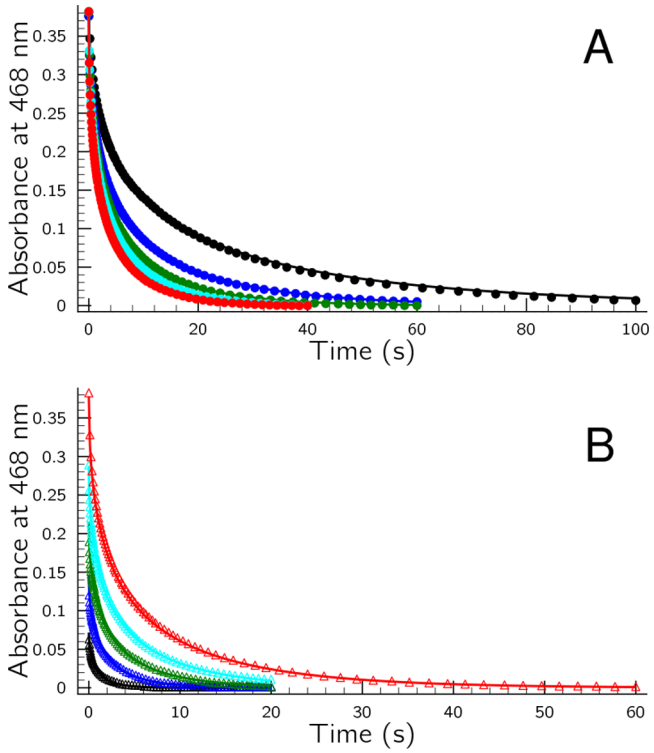

Figure 4. (A) Measured (filled circles) and calculated (solid lines) absorbance−time profiles with varying the initial concentration of methionine at pH = 1.60 and $T_{I_2}^0$ = 0.50 mM in the absence of initially added iodide. Other conditions are as follows: $[Met]_0$/mM = 5.0 (black), 10.0 (blue), 15.0 (green), 20.0 (cyan), and 25.0 (red). (B) Measured (empty triangles) and calculated (solid lines) absorbance−time profiles with varying the initial concentration of iodine at pH = 1.60 and $[Met]_0$ = 15.0 mM in the absence of initially added iodide. Other conditions are as follows: $T_{I_2}^0$/mM = 0.106 (black), 0.193 (blue), 0.285 (green), 0.390 (cyan), 0.500 (red). These curves are obtained by stopped-flow equipment.

$$-\frac{dT_{I_2}}{dt} = k_{app}\frac{[Met][I_2]}{[I^-]} \quad (3)$$

At each pH, the apparent rate coefficients were averaged and these average values were plotted against the hydrogen ion concentration as seen in Figure 5. We would like to emphasize that all the kinetic traces were analyzed regardless of the initial concentration of iodide ion applied. The average deviation obtained for all the 151 kinetic traces were found to be 0.9% which shows an excellent agreement between the measured and calculated data. A clearly nonlinear hydrogen dependence of k_{app} is observed, and the average values of k_{app} can be interpreted by the following empirical formula

$$k_{app} = \frac{A[H^+]^2 + B[H^+] + C}{D[H^+]^2 + E[H^+] + 1} \quad (4)$$

where A = 1075.6 ± 89.6 M^{-2} s^{-1}, B = 149.75 ± 12.35 M^{-1} s^{-1}, C = 0.32409 ± 0.02657 s^{-1}, D = 696402 ± 6168 M^{-2}, and E = 3845.3 ± 34.1 M^{-1} were used. This result is completely consistent with the log−log plot of the initial rate against the hydrogen ion concentration (see Figure 3). Later, we shall see how these values may be rationalized in terms of the rate coefficients calculated from simultaneous data evaluation.

Proposed Kinetic Model for Simultaneous Evaluation of Kinetic Curves. There are three possible options to explain

https://dx.doi.org/10.1021/acs.jpca.0c04271
J. Phys. Chem. A 2020, 124, 6029−6038

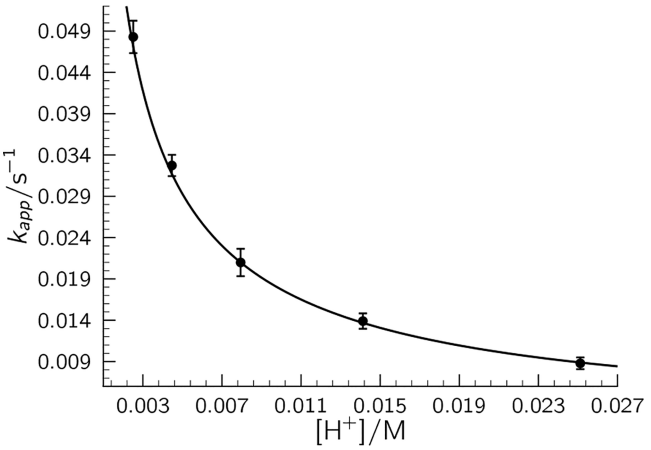

Figure 5. Plot of the averages of k_{app} apparent rate coefficient values obtained by the individual curve fitting method at different pHs against the hydrogen ion concentration. Error bars indicate the standard deviation of the average of k_{app} values calculated at each pH.

the autoinhibitory effect of iodide ion in the title reaction. Probably the simplest one is when we consider the following two-step mechanistic possibility

$$I_2 + I^- \rightleftharpoons I_3^- \quad (5)$$

$$Met + I_2 + H_2O \rightarrow Met{-}SO + 2H^+ + 2I^- \quad (6)$$

when triiodide is treated as a completely inert species, and the rate of eq 6 is linearly proportional to the concentration of both reactants. Evidently, this model has a serious drawback not to take the pH dependence of the kinetic curves into account, but theoretically the iodide inhibition may be encountered. The average deviation for all the 151 experimental traces was found to be 25% clearly indicating that the model has to be improved. Therefore, in the next trial, we have removed eq 6 and inserted the following steps to eq 5:

$$I_2 + H_2O \rightleftharpoons HOI + I^- + H^+ \quad (7)$$

$$Met + HOI \rightarrow Met{-}SO + H^+ + I^- \quad (8)$$

As it is seen, hypoiodous acid here is considered to be the lone reactive species. Because eq 7 is established relatively rapidly and follows the law of mass action type kinetics, an increase in iodide and hydrogen ion concentrations would shift this equilibrium to the left; hence, the overall rate of reaction would decrease giving rise to the inhibitory effect of iodide and hydrogen ions found experimentally. The rate coefficients of the forward and reverse reactions are well-established; therefore, they were used as fixed values (presented later in Table 2) during the whole calculation process.[47−49] Simultaneous evaluation of all the kinetic traces led to 11% average deviation, but removal of the experimental curves measured in the absence of initially added iodide ion would lead to an 2.5% acceptable average deviation. Even the rate coefficients of eq 8 for the rate equation being established as $v = k_1^{HOI}[Met][HOI] + k_2^{HOI}[Met][HOI][H^+]$ may be calculated ($k_1^{HOI} = 2.44 \times 10^8$ M^{-1} s^{-1} and $k_2^{HOI} = 8.0 \times 10^9$ $M^{-2}s^{-1}$) within the reasonable diffusion controlled range. Despite these promising results, we concluded that the above-mentioned model still contains systematic errors suggesting further improvements with a special focus on the kinetic curves measured in the absence of initially added iodide ion. As a final step, we, therefore, propose that eqs 5 and 7 have to be augmented with the following steps for adequate description of the kinetic data measured in this system:

$$Met \rightleftharpoons H^+ + MetH_{-1} \quad (9)$$

$$Met + I_2 \rightleftharpoons Met{-}SI^+ + I^- \quad (10)$$

$$Met{-}SI^+ + H_2O \rightarrow Met{-}SO + I^- + 2H^+ \quad (11)$$

$$MetH_{-1} + I_2 \rightleftharpoons Met{-}SI + I^- \quad (12)$$

$$Met{-}SI + H_2O \rightarrow Met{-}SO + I^- + H^+ \quad (13)$$

where $MetH_{-1}$ is the deprotonated form of methionine. The proposed kinetic model with the rate coefficients fixed and

Table 2. Rate Equations Fixed and Obtained from Evaluating Simultaneously the Kinetic Data of the Methionine−Iodine Reaction[a]

no.	step	rate equation	rate coefficient
(E1)	$H_3PO_4 \rightleftharpoons H^+ + H_2PO_4^-$	$k_{E1}[H_3PO_4]$	1.585×10 s^{-1}
(−E1)		$k_{-E1}[H^+][H_2PO_4^-]$	10^7 M^{-1} s^{-1}
(E2)	$Met \rightleftharpoons H^+ + MetH_{-1}$	$k_{E2}[Met]$	5.248×10^5 s^{-1}
(−E2)		$k_{-E2}[H^+][MetH_{-1}]$	10^8 M^{-1} s^{-1}
(R1)	$I_2 + I^- \rightleftharpoons I_3^-$	$k_{R1}[I_2][I^-]$	5.7×10^9 M^{-1} s^{-1}
(−R1)		$k_{-R1}[I_3^-]$	8.5×10^6 s^{-1}
(R2)	$I_2 + H_2O \rightleftharpoons H^+ + I^- + HOI$	$k_{R2}[I_2]$	5.52×10^{-2} s^{-1}
		$k'_{R2}[I_2]/[H^+]$	1.98×10^{-3} M s^{-1}
(−R2)		$k_{-R2}[H^+][I^-][HOI]$	1.023×10^{11} $M^{-2}s^{-1}$
		$k'_{-R2}[I^-][HOI]$	3.67×10^9 M^{-1} s^{-1}
(R3)	$Met + I_2 \rightleftharpoons Met{-}SI^+ + I^-$	$k_{R3}[Met][I_2]$	370 M^{-1} s^{-1}
(−R3)		$k_{-R3}[Met{-}SI^+][I^-]$	10^6 M^{-1} s^{-1}
(R4)	$Met{-}SI^+ + H_{2O} \rightarrow Met{-}SO + I^- + 2H^+$	$k_{R4}[Met{-}SI^+]$	4.18 ± 0.07 s^{-1}
		$k'_{R4}[Met{-}SI^+]/[H^+]$	0.582 ± 0.007 M s^{-1}
(R5)	$MetH_{-1} + I_2 \rightleftharpoons MetH_{-1}{-}SI + I^-$	$k_{R5}[MetH_{-1}][I_2]$	370 M^{-1} s^{-1}
(−R5)		$k_{-R5}[MetH_{-1}{-}SI][I^-]$	10^6 M^{-1} s^{-1}
(R6)	$MetH_{-1}{-}SI + H_2O \rightarrow Met{-}SO + H^+ + I^-$	$k_{R6}[MetH_{-1}{-}SI]/[H^+]$	0.240 ± 0.002 M s^{-1}

[a]Those rate coefficients where no standard deviation is given are fixed during the whole calculation process.

https://dx.doi.org/10.1021/acs.jpca.0c04271
J. Phys. Chem. A 2020, 124, 6029−6038

determined in the simultaneous evaluation procedure along with the proposed rate equations are visualized in Table 2.

The average deviation for all the 151 kinetic curves was found to be 1.3% indicating a sound agreement between the measured and fitted data. Figures 4 and Figures 6–9 inevitably

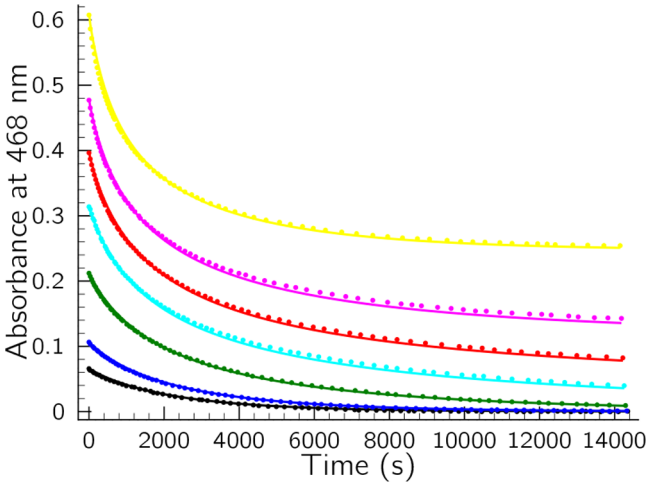

Figure 6. Measured (dots) and calculated (solid lines) absorbance–time profiles with varying the initial concentration of iodine at pH = 1.6 and $[Met]_0$ = 0.48 mM in the presence of initially added iodide ($[I^-]_0$ = 3.0 mM). $T_{I_2}^0$/mM = 0.0877 (black), 0.141 (blue), 0.282 (green), 0.418 (cyan), 0.529 (red), 0.636 (magenta), and 0.810 (yellow).

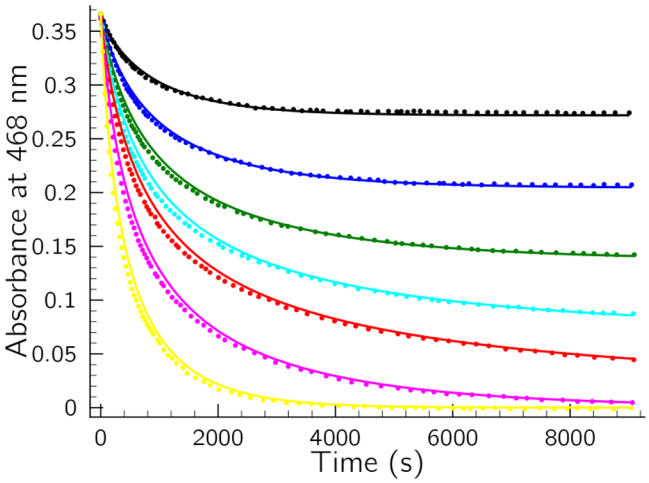

Figure 7. Measured (dots) and calculated (solid lines) absorbance–time profiles with varying the initial concentration of methionine at pH = 2.1 and $T_{I_2}^0$ = 0.485 mM in the presence of initially added iodide ($[I^-]_0$ = 3.0 mM). $[Met]_0$/mM = 0.120 (black), 0.210 (blue), 0.300 (green), 0.390 (cyan), 0.480 (red), 0.720 (magenta), and 1.20 (yellow).

demonstrate that the model is working correctly in the absence and presence of initially added iodide ion, and it is able to describe the effect of initial methionine, iodine concentration, as well as that of pH on the experimental curves.

DISCUSSION

Validation of the Kinetic Parameters. Step E1 is only an auxiliary process that takes the slight pH change into consideration during the whole calculation procedure. Because

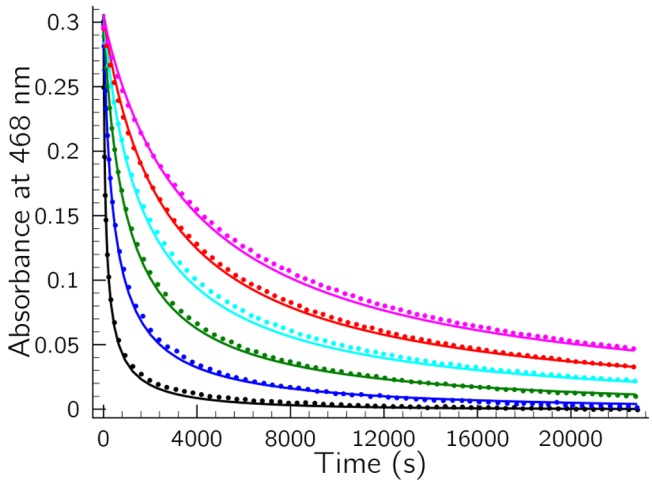

Figure 8. Measured (dots) and calculated (solid lines) absorbance–time profiles with varying the initial iodide concentrations at pH = 2.60 and at $[Met]_0$ = 0.72 mM and $T_{I_2}^0$ = 0.410 mM. $[I^-]_0$/mM = 1.0 (black), 3.0 (blue), 5.0 (green), 7.0 (cyan), 9.0 (red), 11.0 (magenta).

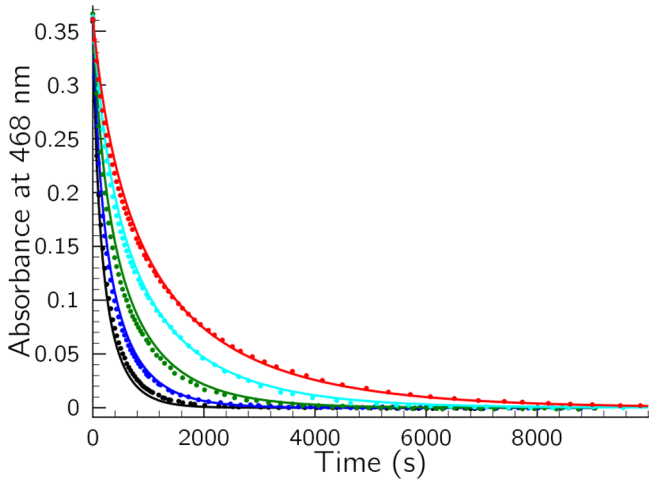

Figure 9. Measured (dots) and calculated (solid lines) absorbance–time profiles with varying the pH at $[Met]_0$ = 1.20 mM and $T_{I_2}^0$ = 0.48 mM in the presence of initially added iodide ion ($[I^-]_0$ = 3.0 mM). pH = 2.6 (black), 2.35 (blue), 2.1 (green), 1.85 (cyan), 1.6 (red).

this equilibrium is established instantaneously, the rate coefficients of both the forward and reverse reactions are fixed to relatively large values, $k_{E1} = 1.585 \times 10^5$ s^{-1} and $k_{-E1} = 10^7$ M^{-1} s^{-1}, respectively. The ratio of these rate coefficients provides the pK_{a1} of phosphoric acid to be 1.8.[42] This value worked consistently well in a number of previous systems investigated.[50−54]

Step E2 is the acid dissociation constant of methionine, which is a rapidly established equilibrium. The rate coefficients of the forward and reverse processes are fixed to be $k_{E2} = 5.248 \times 10^5$ s^{-1} and $k_{-E2} = 10^8$ M^{-1} s^{-1}, respectively. The ratio of these rate coefficients gives the pK_{a1} of methionine to be 2.28.[42] This value along with the pH range studied suggests that Step E2 would indeed be an inevitable process to be considered to describe the measured absorbance–time series.

Step R1 is the well-known rapidly established equilibrium between iodine and triiodide ion studied comprehensively by independent research groups.[55,56] The individual rate co-

https://dx.doi.org/10.1021/acs.jpca.0c04271
J. Phys. Chem. A 2020, 124, 6029−6038

efficients of the forward and backward processes were fixed during the whole calculation procedure as $k_{R1} = 5.7 \times 10^9$ M^{-1} s^{-1} and $k_{-R1} = 8.5 \times 10^6$ s^{-1}, respectively, to provide $\log\beta_{I_3^-} = 2.83$, where $\beta_{I_3^-}$ is the formation constant of triiodide ion.

Step R2 is the well-established hydrolytic equilibrium of iodine studied thoroughly decades ago. The rate coefficients of the forward and backward processes including the H^+-inhibited pathway were determined previously,[47−49] and these rate coefficients were directly adopted here. Because this equilibrium is established relatively rapidly under our experimental circumstances, it enables us to eliminate H_2OI^+ species from the model. Consequently, the rate coefficient of k_{-R2} was recalculated from the values reported by Lengyel et al.[49] The fixed rate coefficients used throughout the whole calculation process are indicated in Table 2.

Step R3 was already suggested by Chikwana et al.,[32] where iodonium ion transfer is considered to take place on the nonbonding electron pair of the inner sulfur atom in a rapid preequilibrium. This kind of heterolytic transfer process seems to be a general phenomenon of iodine oxidation reactions when I_2 attacks an inner sulfur atom of a substrate molecule.[57−59] Our calculation confirmed that the title reaction is initiated by this equilibrium. We have systematically checked as well whether either of these individual rate coefficients may be obtained from our experiments or not. Our preliminary calculation showed that set of k_{R3}, k_{-R3}, k_{R4} and that of k_{R3}, k_{-R3}, k_{R4}' are in total correlation, therefore these individual rate coefficients cannot be determined independently. As a first step we have fixed k_{-R3} and performed a series of calculations with varying k_{R3}, k_{R4}, and k_{R4}'. These calculations showed that any value higher than $k_{-R3} = 10^6$ M^{-1} s^{-1} would lead to the same average deviation; therefore, we have fixed k_{-R3} to this lower limit value and tried to determine k_{R3}. Unfortunately, k_{R3} was also found to be strongly correlated with k_{R4} and k_{R4}'. Systematic analysis of calculation series has revealed that when k_{R3} is between 300 and 500 M^{-1} s^{-1}, then the average deviation in the case of all the 151 kinetic traces would lead to 1.3−1.4% average deviation, but outside this region, it increases significantly indicating systematic deviations between the measured and calculated data. Therefore, we have fixed $k_{R3} = 370$ M^{-1} s^{-1} and determined k_{R4} and k_{R4}'. It means that a low value of $K_{R3} = k_{R3}/k_{-R3} = 3.7 \times 10^{-4}$ may be calculated for the equilibrium constant of Step R3. Later, we shall see that it provides such parametric conditions that Met−SI^+ can be treated as short-lived intermediate with having a small steady-state concentration value for this species. For the sake of completeness, it should also be mentioned that Young and Hsieh[40] came to a conclusion that the methionine−iodine reaction is subject to general base catalysis because at low buffer concentration the reaction rate is inversely dependent on the iodide concentration but at high buffer concentrations it shows nonlinear dependence. This observation is explained by the formation of a tetracoordinated sulfurane species. We have therefore performed series of experiments with varying the buffer components concentration but found no observable effect as seen in Figure S3 of the Supporting Information. From these experiments we have concluded that buffer component concentration change, keeping the rest of the conditions constant, does not affect the kinetic traces, thus at least under our experimental conditions the general base catalysis seems to be dubious. It is interesting to note, however, that changing kinetic order of iodide ion is confirmed in our present experiments as well, but this phenomenon is rather related to the varying iodide concentration but not to the alteration of buffer concentration. It appears to suggest that iodide impurities might have played a notable role in Young and Hsieh experiments.

Step R4 is the hydrolysis of Met−SI^+ formed in the preequilibrium. We have also found that the rate of this process must contain two terms, the first one has to be independent of pH and the second one is inversely proportional to $[H^+]$. The inclusion of the latter pathway is experimentally verified by the pH dependence of the kinetic curves seen in Figure 9. After fixing $k_{R3} = 370$ M^{-1} s^{-1} and $k_{-R3} = 10^6$ M^{-1} s^{-1}, we could calculate $k_{R4} = 10.9 \pm 0.2$ s^{-1} and $k_{R4}' = 0.350 \pm 0.005$ M s^{-1}, which means that only $k_{R3}k_{R4}/k_{-R3} = 4.033 \times 10^{-3}$ s^{-1} and $k_{R3}k_{R4}'/k_{-R3} = 1.295 \times 10^{-4}$ M s^{-1} can be determined unambiguously from our experiments, with some restrictions that $k_{-R3} \geq 10^6$ M^{-1} s^{-1} and $300 \leq k_{R3} \leq 500$ M^{-1} s^{-1} inequalities have to be fulfilled.

Step R5 is also an iodonium ion transfer process that occurs between the deprotonated form of methionine and iodine. Neither the individual rate coefficient of the forward process nor that of the reverse reaction can unambiguously be determined from our experiments. Therefore, we fixed $k_{R5} = 370$ M^{-1} s^{-1} and $k_{-R5} = 10^6$ M^{-1} s^{-1} throughout the calculation process.

Step R6 is the rapid hydrolysis of $MetH_{-1}$−SI, and its rate coefficient may be calculated if k_{R5} and k_{-R5} are fixed. Our calculation has revealed that $k_{R6} = 0.240 \pm 0.002$ M s^{-1}, but actually $K_{R5}k_{R6} = 8.88 \times 10^{-5}$ M s^{-1} can be determined unambiguously from our experiments.

Interpretation of the Results. As it was already mentioned Met−SI^+ and $MetH_{-1}$−SI are a short-lived intermediates; therefore, their steady state concentrations may be obtained from the following equations

$$\frac{d[Met-SI^+]}{dt} = k_{R3}[Met][I_2] - k_{-R3}[Met-SI^+][I^-] - (k_{R4} + k_{R4}'/[H^+])[Met-SI^+] \quad (14)$$

$$\frac{d[MetH_{-1}-SI]}{dt} = k_{R5}[MetH_{-1}][I_2] - k_{-R5}[MetH_{-1}-SI][I^-] - k_{R6}/[H^+][MetH_{-1}-SI] \quad (15)$$

leading to the following steady-state concentrations

$$[Met-SI^+] = \frac{k_{R3}[Met][I_2]}{k_{-R3}[I^-] + (k_{R4} + k_{R4}'/[H^+])} \quad (16)$$

$$[MetH_{-1}-SI] = \frac{k_{R5}[MetH_{-1}][I_2]}{k_{-R5}[I^-] + k_{R6}/[H^+]} \quad (17)$$

Because the consumption of total amount of iodine (and methionine) can be described by the following differential equation

$$-\frac{dT_{Met}}{dt} = -\frac{dT_{I_2}}{dt} = k_{R3}[Met][I_2] - k_{-R3}[Met-SI^+][I^-] + k_{R5}[MetH_{-1}][I_2] - k_{-R5}[MetH_{-1}-SI][I^-] \quad (18)$$

substitution of eqs 16 and 17 into eq 18 followed by some algebraic rearrangements and simplifications leads to

https://dx.doi.org/10.1021/acs.jpca.0c04271
J. Phys. Chem. A 2020, 124, 6029−6038

$$-\frac{dT_{I_2}}{dt} = k_{app}\frac{T_{Met}[I_2]}{[I^-]} \quad (19)$$

where

$$k_{app} = \frac{\frac{k_{R3}k_{R4}k_{-R5}[I^-]}{K_{E2}(k_{-R3}k_{R6}+k_{R4}'k_{-R5})}[H^+]^2 + \frac{k_{R3}k_{R4}'k_{-R5}[I^-]}{K_{E2}(k_{-R3}k_{R6}+k_{R4}'k_{-R5})}[H^+] + \frac{k_{-R3}k_{R5}k_{R6}K_{E2}[I^-]}{K_{E2}(k_{-R3}k_{R6}+k_{R4}'k_{-R5})}}{\frac{k_{-R3}k_{-R5}[I^-]+k_{R4}k_{-R5}}{K_{E2}(k_{-R3}k_{R6}+k_{R4}'k_{-R5})}[H^+]^2 + \frac{k_{-R3}k_{-R5}K_{E2}[I^-]+k_{R4}k_{-R5}K_{E2}+k_{-R3}k_{R6}+k_{R4}'k_{-R5}}{K_{E2}(k_{-R3}k_{R6}+k_{R4}'k_{-R5})}[H^+] + 1} \quad (20)$$

From this equation, it is easy to realize that A, B, C, D, and E in eq 4 may easily be expressed in terms of the rate coefficients obtained and that of initial iodide concentration used in the majority of experiments. Using the above-mentioned rate coefficients presented in Table 2 and $[I^-]_0 = 3.0$ mM, one can easily calculate $A = 1072.95\ M^{-2}\ s^{-1}$, $B = 149.65\ M^{-1}\ s^{-1}$, $C = 0.32465\ s^{-1}$, $D = 694712\ M^{-2}$, and $E = 3836.4\ M^{-1}$ to describe averages of k_{app} against the $[H^+]$ obtained from individual evaluation. Another important experimental result regarding the log−log plot of initial rate versus hydrogen ion concentration may also be confirmed by eq 20. To highlight it, the limits of k_{app} at high and low values of $[H^+]$ may be obtained as follows, when $[I^-]_0 = 3.0$ mM is used:

$$\lim_{[H^+]\to 0} k_{app} = C = 0.32465\ s^{-1} \quad (21)$$

and

$$\lim_{[H^+]\to \infty} k_{app} = \frac{A}{D} = 1.544 \times 10^{-3}\ s^{-1} \quad (22)$$

meaning that under these conditions, the initial rate becomes independent of pH as it is manifested in Figure 3.

Finally, we shall also point out, how the formal kinetic order of iodide ion increases up to even −2 as suggested in Figure 3. It is well-known that the $[I_2]$ may easily be expressed by the help total iodine concentration (T_{I_2}) as follows:

$$[I_2] = \frac{T_{I_2}}{1 + K_{R1}[I^-]} \quad (23)$$

where K_{R1} is the formation constant of triiodide ion. Substituting this equation into eq 19 combined with eq 20 followed by some algebraic manipulations leads to the following expression:

$$-\frac{dT_{I_2}}{dt} = k_{app}\frac{T_{Met}T_{I_2}}{[I^-] + K_{R1}[I^-]^2} \quad (24)$$

It is easy to see if $[I^-]_0 \gg 1.5 \times 10^{-3}$ M condition is fulfilled, then the first term in the denominator is negligible; thus, the formal kinetic order of iodide becomes −2 indicating a very efficient autoinhibitory feature.

Last but not least, some words are also in an order here to put a clear emphasis why this detailed investigation was necessary even if the kinetics of this system was already reported in seemingly sufficient details in a recent report by Chikwana et al.[32] in 2009. First, the abstract of the cited paper explicitly says that the direct reaction between iodine and methionine is slow and mildly autoinhibitory. Our results presented here, however, just partially agrees with this statement. The reaction in the absence of initially added iodide ion is fairly rapid (stopped-flow technique is required to follow conveniently the reaction) but indeed autoinhibitory with respect to iodide ion. This autoinhibitory effect is, however, not as mild as stated, at pH = 2 and above, $[I^-]_0 >$ 3.0 mM condition, it is so effective that an order of magnitude increase in the iodide concentration decreases the initial rate by 2 orders of magnitude! This hidden characteristic is indeed the consequence of limited range of initially added iodide ion concentration used in the previous study.[32] Second, it was recently shown by Stanbury[60] that the model, intended to describe the methionine−iodate and methionine−iodine combined system, proposed by these authors extremely violates the principle of detailed balancing by 11(!) orders of magnitude making their mechanism completely unreliable. Third, no pH dependence of the methionine−iodine reaction was suggested by Chikwana et al. at the same pH range where slight pH-dependence should have been observed. For the sake of completeness, we have to admit that it is a bit difficult to realize this effect without systematically focusing the pH region where it appears the most prominently. Fourth, the iodide inhibitory effect of the title system in Chikwana's paper was explained by the concurrent but more sluggish reaction between methionine and triiodide ion compared to the one between methionine and iodine. This model, however, fails to properly describe the measured curves in excess of methionine reported in Chikwana's article (see Figure 8a of ref 32 compared to Figure S2 of the Supporting Information).

CONCLUSION

Significant improvement of the kinetic model of the methionine−iodine reaction, which was designated to be the key process of the methionine−iodate system, is presented here to provide a meaningful assistance for adequately describing the clock characteristics of the parent reaction. It was clearly shown that the strong autoinhibitory feature of iodide ion may be observed even at its relatively low concentration. At the same time, mild hydrogen ion dependence of its rate reveals that among the I-containing species, iodine is the kinetically active form. A simple seven-step kinetic model is proposed to describe all of the most important characteristics of the kinetic curves measured from which a rate equation may as well be derived. Last but not least, this work provides a strong warning flag in a sense that even a seemingly simple reaction has to be studied with special circumspection to establish a reliable model to avoid misinterpretation of the dynamics of a more complex system where the given mechanism is believed to play a crucial role.

ASSOCIATED CONTENT

Supporting Information

The Supporting Information is available free of charge at https://pubs.acs.org/doi/10.1021/acs.jpca.0c04271.

Tables including the composition of kinetic runs and the stoichiometric ratios in excess of iodine as well as figures on the reproduction of the measured and simulated kinetic curves by the model suggested by Chikwana et al. published in ref 32 (PDF)

https://dx.doi.org/10.1021/acs.jpca.0c04271
J. Phys. Chem. A 2020, 124, 6029−6038

AUTHOR INFORMATION

Corresponding Author

Attila K. Horváth − *Department of Inorganic Chemistry, Faculty of Sciences, University of Pécs, Pécs, Hungary H-7624;* orcid.org/0000-0002-1916-2451; Email: horvatha@gamma.ttk.pte.hu

Authors

Li Xu − *Department of Chemical Engineering and Technology, School of Chemistry, Biology and Material of Science, East China University of Technology, Nanchang 330013, Jiangxi Province, People's Republic of China*

György Csekő − *Department of Inorganic Chemistry, Faculty of Sciences, University of Pécs, Pécs, Hungary H-7624*

Complete contact information is available at: https://pubs.acs.org/10.1021/acs.jpca.0c04271

Notes

The authors declare no competing financial interest.

ACKNOWLEDGMENTS

This work was as well supported by the GINOP-2.3.2-15-2016-00049 grant. The study was also financed by the Higher Education Institutional Excellence Programme of the Ministry of Innovation and Technology in Hungary, within the framework of the innovation for sustainable and healthy living and environment thematic programme of the University of Pécs. The project has been supported by the European Union, cofinanced by the European Social Fund Grant No. EFOP-3.6.1.-16-2016-00004 entitled by Comprehensive Development for Implementing Smart Specialization Strategies at the University of Pécs. Financial support of the Hungarian Research Fund NKFIH-OTKA Grant No. K116591 is also acknowledged. This work was also supported by the Start-up Funding (Grant No. DHBK2017163) from East China University of Technology. The authors are grateful to Dr. Attila Takács for his helpful assistance in the ^{1}H NMR measurements.

REFERENCES

(1) Atmaca, G. Antioxidant Effects of Sulfur-containing Amino Acids. *Yonsei Med. J.* **2004**, *45*, 776−778.

(2) Piste, P. Cysteine-master Antioxidant. *Int. J. Pharm. Chem. Biol. Sci.* **2013**, *3*, 143−149.

(3) Ren, W.; Li, Y.; Yin, Y.; Blachier, F. In *Nutritional and Physiological Functions of Amino Acids in Pigs*; Blachier, F., Wu, G., Yin, Y., Eds.; Springer: Vienna, Austria, 2013; pp 91−108.

(4) He, Q.; Yin, Y.; Zhao, F.; Kong, X.; Wu, G.; Ren, P. Metabonomics and its Role in Amino Acid Nutrition Research. *Front. Biosci., Landmark Ed.* **2011**, *16*, 2451−2460.

(5) Kim, J. H.; Jang, H. J.; Cho, W. Y.; Yeon, S. J.; Lee, C. H. In vitro Antioxidant Actions of Sulfur-containing Amino Acids. *Arabian J. Chem.* **2020**, *13*, 1678−1684.

(6) Shendikova, E. N.; Mel'sitova, I. V.; Yurkova, I. L. Effect of Sulfur-containing Amino Acids and Peptides on the Free-radical Fragmentation of Biologically Active Phospho Derivatives of Glycerol. *High Energy Chem.* **2017**, *51*, 363−368.

(7) Bin, P.; Huang, R.; Zhou, X. Oxidation Resistance of the Sulfur Amino Acids: Methionine and Cysteine. *BioMed Res. Int.* **2017**, *2017*, 958493.

(8) Martinez, Y.; Li, X.; Liu, G.; Bin, P.; Yan, W.; Mas, D.; Valdivie, M.; Hu, C.-A. A.; Ren, W.; Yin, Y. The Role of Methionine on Metabolism, Oxidative Stress, and Diseases. *Amino Acids* **2017**, *49*, 2091−2098.

(9) Brosnan, J. T.; Brosnan, M. E. The Sulfur-containing Amino Acids: an Overview. *J. Nutr.* **2006**, *136*, 1636S−1640S.

(10) Bittle, J.; Menezes, E. C; McCormick, M. L; Spitz, D. R; Dailey, M.; Stevens, H. E The Role of Redox Dysregulation in the Effects of Prenatal Stress on Embryonic Interneuron Migration. *Cereb. Cortex* **2019**, *29*, 5116−5130.

(11) Townsend, D. M.; Tew, K. D.; Tapiero, H. Sulfur Containing Amino Acids and Human Disease. *Biomed. Pharmacother.* **2004**, *58*, 47−55.

(12) Zheng, Y.; Ritzenthaler, J. D.; Burke, T. J.; Otero, J.; Roman, J.; Watson, W. H. Age−dependent Oxidation of Extracellular Cysteine/Cystine Redox State (E(Cys/Cyss)) in Mouse Lung Fibroblasts Is Mediated by a Decline in SIc7a11 Expression. *Free Radical Biol. Med.* **2018**, *118*, 13−22.

(13) Cholkar, K.; Veeranki, S.; Puttaswamy, P.; Anand, S.; Made Gowda, N. M. Kinetics and Mechanism of Oxidative Conversion of Methionine to Sulfone by Chloramine-B in Acid Medium. *Curr. Phys. Chem.* **2018**, *8*, 37−45.

(14) Mackay, D. S.; Brophy, J. D.; Mcbreairty, L. E.; Mcgowan, R. A.; Bertolo, R. F. Intrauterine Growth Restriction Leads to Changes in Sulfur Amino Acid Metabolism, but Not Global DNA Methylation. Yucatan Miniature Piglets. *J. Nutr. Biochem.* **2012**, *23*, 1121−1127.

(15) Lim, J. M.; Kim, G.; Levine, R. L. Methionine in Proteins: It's Not Just for Proteine Initiation Anymore. *Neurochem. Res.* **2019**, *44*, 247−257.

(16) Campbell, K.; Vowinckel, J.; Keller, M. A.; Ralser, M. Methionine Metabolism Alters Oxidative Stress Resistance via the Pentose Phosphate Pathway. *Antioxid. Redox Signaling* **2016**, *24*, 543−547.

(17) Liu, G.; Yu, L.; Fang, J.; Hu, C. A.; Yin, J.; Ni, H.; Ren, W.; Duraipandiyan, V.; Chen, S.; Al-Dhabi, N. A.; et al. Methionine Restriction on Oxidative Stress and Immune Response in Dss-Induced Colitis Mice. *Oncotarget* **2017**, *8*, 44511−44520.

(18) Veredas, F. J.; Cantón, F. R.; Aledo, J. C. Methionine Residues Around Phosphorylation Sites Are Preferentially Oxidized in vivo Under Stress Conditions. *Sci. Rep.* **2017**, *7*, 40403.

(19) Kovačević, G.; Ostafe, R.; Fischer, R.; Prodanović, R. Influence of Methionine Residue Position on Oxidative Stability of Glucose Oxidase from Sergillus Niger. *Biochem. Eng. J.* **2019**, *146*, 143−149.

(20) Walker, E. J.; Bettinger, J. Q.; Welle, K. A.; Hryhorenko, J. R.; Ghaemmaghami, S. Global Analysis of Methionine Oxidation Provides a Census of Folding Stabilities for the Human Proteome. *Proc. Natl. Acad. Sci. U. S. A.* **2019**, *116*, 6081−6090.

(21) Takahashi, Y.; Taki, Y.; Takeda, K.; Hashizume, H.; Tanaka, H.; Ishikawa, K.; Hori, M. Reduced HeLa Cell Viability in Methionine-containing Cell Culture Medium Irradiated with Microwave-excited Atmospheric-pressure Plasma. *Plasma Processes Polym.* **2018**, *15*, 1700200.

(22) Kim, H. Y. The Methionine Sulfoxide Reduction System: Selenium Utilization and Methionine Sulfoxide Reductase Enzymes and Their Functions. *Antioxid. Redox Signaling* **2013**, *19*, 958−969.

(23) Chandler, J. D.; Margaroli, C.; Horati, H.; Kilgore, M. B.; Veltman, M.; Liu, H. K.; Taurone, A. J.; Peng, L.; Guglani, L.; Uppal, K.; et al. Myeloperoxidase Oxidation of Methionine Associates with Early Cystic Fibrosis Lung Disease. *Eur. Respir. J.* **2018**, *52*, 1801118.

(24) Nimse, S. B.; Pal, D. Free Radical, Natural Antioxidants, and Their Reaction Mechanisms. *RSC Adv.* **2015**, *5*, 27986−28006.

(25) Lockhart, C.; Smith, A. K.; Klimov, D. K. Methionine Oxidation Changes the Mechanism of Aβ Peptide Binding to the DMPC Bilayer. *Sci. Rep.* **2019**, *9*, 5947.

(26) Gu, S. X.; Stevens, J. W.; Lentz, S. R. Regulation of Thrombosis and Vascular Function by Protein Methionine Oxidation. *Blood* **2015**, *125*, 3851−3859.

(27) Soares, M. S. P.; Oliveira, P. S.; Debom, G. N.; da Silveira Mattos, B.; Polachini, C. R.; Baldissarelli, J.; Morsch, V. M.; Schetinger, M. R. C.; Tavares, R. G.; Stefanello, F. M.; Spanevello, R. M.; et al. Chronic Administration of Methionine and/or Methionine Sulfoxide Alters Oxidative Stress Parameters and ALA-

D Activity in Liver and Kidney of Young Rats. *Amino Acids* **2017**, *49*, 129−138.
(28) Mansour, M. A. Kinetics and Mechanims of Chromium(VI) Oxidation of L-Methionine. *Transition Met. Chem.* **2002**, *27*, 818−821.
(29) Sumathi, T.; Shanmugasundaram, P.; Chandramohan, G. A Kinetic and Mechanistic Study on the Oxidation of L-Methionine and N-Acetyl L-Methionine by Cerium(IV) in Sulfuric Acid Medium. *Arabian J. Chem.* **2016**, *9*, S177−S184.
(30) Chidankumar, C. S.; Chandraju, S.; Made Gowda, N. M. Manganese(III) Oxidation of L-Methionine in Aqueous Acetic Acid Medium: a Kinetic and Mechanistic Study. *Synth. React. Inorg., Met.-Org., Nano-Met. Chem.* **2009**, *39*, 645−650.
(31) Armesto, X.L.; Canle L, M.; Fernandez, M.I.; Garcıa, M.V.; Santaballa, J.A. First Steps in the Oxidation of Sulfur-containing Amino Acids by Hypohalogenation: Very Fast Generation of Intermediate Sulfenyl Halides and Halosulfonium cations. *Tetrahedron* **2000**, *56*, 1103−1109.
(32) Chikwana, E.; Davis, B.; Morakinyo, M. K.; Simoyi, R. H. Oxyhalogen-Sulfur Chemistry−Kinetic and Mechanism of Oxidation of Methionine by Aqueous Iodine and Acidified Iodate. *Can. J. Chem.* **2009**, *87*, 689−697.
(33) Idris, S. O.; Ibrahim, A. P.; Iyun, J. F.; Mohammed, Y. Kinetics and Mechanism of Oxidation of L-Methionine by Potassium Bromate in Aqueous Hydrochloric Acid Medium. *Arch. Applied Sci. Res.* **2010**, *2*, 355−362.
(34) Sjöberg, B.; Foley, S.; Cardey, B.; Fromm, M.; Enescu, M. Methionine Oxidation by Hydrogen Peroxide in Peptides and Proteins: a Theoretical and Raman Spectroscopy Study. *J. Photochem. Photobiol., B* **2018**, *188*, 95−99.
(35) Pilkington, A. W.; Donohoe, G. C.; Akhmedov, N. G.; Ferrebee, T.; Valentine, S. J.; Legleiter, J. Hydrogen Peroxide Modifies Aβ−Membrane Interactions with Implications for Aβ_{40} Aggregation. *Biochemistry* **2019**, *58*, 2893−2905.
(36) Marino, T.; Soriano-Correa, C.; Russo, N. Oxidation Mechanism of Methionine by HO· Radical: a Theoretical Study. *J. Phys. Chem. B* **2012**, *116*, 5349−5354.
(37) Gangwani, H.; Sharma, P. K.; Banerji, K. K. Kinetics and Mechanism of Oxidation of Methionine by Hexamethylenetetramine-Bromine. *Int. J. Chem. Kinet.* **2000**, *32*, 615−622.
(38) Pandeeswaran, M.; Bincy, J.; Bhuvaneshwari, D.S.; Elango, K.P. Kinetics and Mechanism of the Oxidation of Methionine by Quinolinium Chlorochromate. *J. Serb. Chem. Soc.* **2005**, *70*, 145−151.
(39) Goyal, A.; Kothari, S. Kinetics and Mechanism of the Oxidation of Methionine by Benzyltrimethylammonium Tribromide. *Indian J. Chem.* **2003**, *42B*, 2129−2132.
(40) Young, P. R.; Hsieh, L. S. General Base Catalysis and Evidence for a Sulfurane Intermediate in the Iodine Oxidation of Methionine. *J. Am. Chem. Soc.* **1978**, *100*, 7121−7122.
(41) Diculescu, V. C.; Enache, T. A. Voltammetric and Mass Spectrometry Investigation of Methionine Oxidation. *J. Electroanal. Chem.* **2019**, *834*, 124−129.
(42) *IUPAC Stability Constant Database*, Royal Society of Chemistry: London, 1992−1997.
(43) Tonomura, B.; Nakatani, H.; Ohnishi, M.; Yamaguchi-Ito, J.; Hiromi, K. Test Reactions for a Stopped-Flow Apparatus: Reduction of 2,6-dichlorophenolindophenol and Potassium Ferricyanide by L-ascorbic Acid. *Anal. Biochem.* **1978**, *84*, 370−383.
(44) Gottlieb, H. E.; Kotlyar, V.; Nudelman, A. NMR Chemical Shifts of Common Laboratory Solvents as Trace Impurities. *J. Org. Chem.* **1997**, *62*, 7512−7515.
(45) Peintler, G. *ChemMech/ZiTa: A Comprehensive Program Package for Fitting Parameters of Chemical Reaction Mechanism*; Attila József University: Szeged, Hungary, 1989−2011.
(46) Rábai, G.; Beck, M. T. Oxidation of Thiourea by Iodate: a New Type of Oligo-Oscillatory Reaction. *J. Chem. Soc., Dalton Trans.* **1985**, 1669−1672.
(47) Eigen, M.; Kustin, K. The Kinetics of Halogen Hydrolysis. *J. Am. Chem. Soc.* **1962**, *84*, 1355−1361.
(48) Lengyel, I.; Epstein, I. R.; Kustin, K. Kinetics of Iodine Hydrolysis. *Inorg. Chem.* **1993**, *32*, 5880−5882.
(49) Lengyel, I.; Li, J.; Kustin, K.; Epstein, I. R. Rate Constants for Reactions between Iodine- and Chlorine-Containing Species: A Detailed Mechanism of the Chlorine Dioxide/Chlorite-Iodide Reaction. *J. Am. Chem. Soc.* **1996**, *118*, 3708−3719.
(50) Xu, L.; Horváth, A. K. A Possible Candidate to Be Classified as an Autocatalysis-Driven Clock Reaction: Kinetics of the Pentathionate−Iodate Reaction. *J. Phys. Chem. A* **2014**, *118*, 6171−6180.
(51) Xu, L.; Horváth, A. K. Autocatalysis-Driven Clock Reaction II: Kinetics of the Pentathionate−Periodate Reaction. *J. Phys. Chem. A* **2014**, *118*, 9811−9819.
(52) Csekő, G.; Gao, Q.; Xu, L.; Horváth, A. K. Autocatalysis-Driven Clock Reaction III: Clarifying the Kinetics and Mechanism of the Thiourea Dioxide−Iodate Reaction in an Acidic Medium. *J. Phys. Chem. A* **2019**, *123*, 1740−1748.
(53) Csekő, G.; Gao, Q.; Takács, A.; Horváth, A. K. Exact Concentration Dependence of the Landolt Time in the Thiourea Dioxide−Bromate Substrate-Depletive Clock Reaction. *J. Phys. Chem. A* **2019**, *123*, 3959−3968.
(54) Csekő, G.; Gao, Q.; Pan, C.; Xu, L.; Horváth, A. K. On the Kinetics and Mechanism of the Thiourea Dioxide−Periodate Autocatalysis-Driven Iodine-Clock Reaction. *J. Phys. Chem. A* **2019**, *123*, 7582−7589.
(55) Turner, D. H.; Flynn, G. W.; Sutin, N.; Beitz, J. V. Laser Raman Temperature-Jump Study of the Kinetics of the Triiodide Equilibrium. Relaxation Times in the 10^{-8}−10^{-7} Second Range. *J. Am. Chem. Soc.* **1972**, *94*, 1554−1559.
(56) Ruasse, M.; Aubard, J.; Galland, B.; Adenier, A. Kinetic Study of the Fast Halogen-Trihalide Ion Equilibria in Protic Media by the Raman-Kaser Temperature-Jump Technique. A Non-Diffusion-Controlled Ion−Molecule Reaction. *J. Phys. Chem.* **1986**, *90*, 4382−4388.
(57) Kerek, A.; Horváth, A. K. Kinetics and Mechanism of the Oxidation of Tetrathionate by Iodine in a Slightly Acidic Medium. *J. Phys. Chem. A* **2007**, *111*, 4235−4241.
(58) Csekő, G.; Horváth, A. K. Non-Triiodide Based Autoinhibition by Iodide Ion in the Trithionate−Iodine Reaction. *J. Phys. Chem. A* **2010**, *114*, 6521−6526.
(59) Xu, L.; Csekő, G.; Kégl, T.; Horváth, A. K. General Pathway of Sulfur-Chain Breakage of Polythionates by Iodine Confirmed by the Kinetics and Mechanism of the Pentathionate−Iodine Reaction. *Inorg. Chem.* **2012**, *51*, 7837−7843.
(60) Stanbury, D. M. Comment on the Principle of Detailed Balancing in Complex Mechanisms and Its Application to Iodate Reactions. *J. Phys. Chem. A* **2018**, *122*, 3956−3957.

https://dx.doi.org/10.1021/acs.jpca.0c04271
J. Phys. Chem. A 2020, 124, 6029−6038